Supplementary Material for: "Derivation of coarse-grained simulation models of chlorophyll molecules in lipid bilayers for applications in light harvesting systems"

Ananya Debnath[†] [a], Sabine Wiegand[‡], Harald Paulsen[‡], Kurt Kremer[†], Christine Peter[†] [b]
[†] Max Planck Institute for Polymer Research, 10 Ackermannweg, 55128 Mainz, Germany.
[‡] University of Mainz, Johannes-von-Müller-Weg 6, 55128 Mainz, Germany.

This supplementary material contains:

- additional information regarding the properties of the newly parameterized CG model of chl *b* and *a* in the lipid bilayer as discussed in the main text
- details regarding the probe preparation and interpretation of the FRET experiments of chl aggregation in lipid vesicles

1 CG parameter development

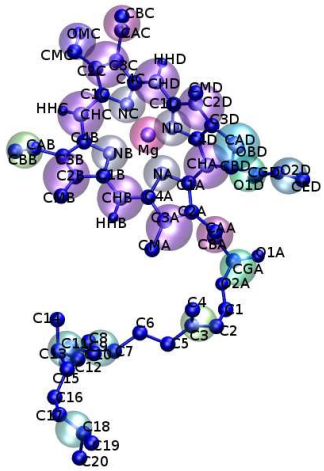

Figure S1 AA bead types for chl *b*.

present affiliation, [a] Department of Chemistry, Indian Institute of Technology Jodhpur, Jodhpur 342011, INDIA
[b] Universität Konstanz, Fachbereich Chemie, Fach 718, D-78457 Konstanz, Germany.

Chl *b*			Chl *a*		
atom	charge group	partial charge	atom	charge group	partial charge
Mg1	1	1	Mg1	1	1.0
NA	1	-0.25	NA	1	-.25
NB	1	-0.25	NB	1	-.25
NC	1	-0.25	NC	1	-.25
ND	1	-0.25	ND	1	-.25
CHA	2	0	CHA	2	0.0
C1A	3	0	C1A	3	0.0
C2A	3	0	C2A	3	0.0
C3A	3	0	C3A	3	0.0
C4A	3	0	C4A	3	0.0
CMA	4	0	CMA	4	0.0
CAA	5	0.4	CAA	5	0.4
CBA	5	0.3	CBA	5	0.3
CGA	5	0.7	CGA	5	.7
O1A	5	-0.7	O1A	5	-.7
O2A	5	-0.7	O2A	5	-.7
CHB	6	-0.1	CHB	6	-.1
HHB	6	0.1	HHB	6	0.1
C1B	7	0	C1B	7	0.0
C2B	7	0	C2B	7	0.0
C3B	7	0	C3B	7	0.0
C4B	7	0	C4B	7	0.0
CMB	8	0	CMB	8	0.0
CAB	9	0	CAB	9	0.0
CBB	9	0	CBB	9	0.0
CHC	10	-0.1	CHC	10	-.1
HHC	10	0.1	HHC	10	0.1
C1C	11	0	C1C	11	0.0
C2C	11	0	C2C	11	0.0
C3C	11	0	C3C	11	0.0
C4C	11	0	C4C	11	0.0
CMC	12	0.25	CMC	12	0.0
CAC	13	0	CAC	13	0.0
CBC	13	0	CBC	13	0.0
CHD	14	-0.1	CHD	14	-.1
HHD	14	0.1	HHD	14	.1
C1D	15	0	C1D	15	0.0
C2D	15	0	C2D	15	0.0
C3D	15	0	C3D	15	0.0
C4D	15	0	C4D	15	0.0
CMD	16	0	CMD	16	0.0
CAD	17	0.25	CAD	17	0.25
CBD	17	0	CBD	17	0.0
CGD	18	0.8	CGD	18	0.8
O1D	18	-0.6	O1D	18	-0.6
O2D	18	-0.7	O2D	18	-0.7
OMC	19	-0.25	OBD	19	-0.25
OBD	20	-0.25	CED	20	0.5
CED	21	0.5			

Table 1 Partial charges for AA Chl *b* and Chl *a*. Remaining beads in the tails (C1 to C20) have zero partial charges.

atom	partial charge
P5N	1.00000
P1N_1	-.25000
P1N_2	-.25000
P1N_3	-.25000
P1N_4	-.25000

Table 2 Partial charges for CG Chl *b* and Chl *a*. Remaining beads have zero partial charges.

AA Chl *b* beads	CG Chl *b* beads	AA Chl *a* beads	CG Chl *a* beads
Mg	P5N	Mg	P5N
NA	P1N_1	NA	P1N_1
NB	P1N_2	NB	P1N_2
NC	P1N_3	NC	P1N_3
ND	P1N_4	ND	P1N_4
C1A,CHA,C4D	SC3_1	C1A,CHA,C4D	SC3_1
C1D,CHD,HHD,C4C	SC3_2	C1D,CHD,HHD,C4C	SC3_2
CAC,CBC	C2_1	CAC,CBC	C2_1
C4B,CHC,C1C,HHC	SC3_3	C4B,CHC,C1C,HHC	SC3_3
CMB,C2B,C3B	SC3_4	CMB,C2B,C3B	SC3_4
CBB,CAB	C3_2	CBB,CAB	C3_2
HHB,CHB,C1B,C4A	SC3_5	HHB,CHB,C1B,C4A	SC3_5
CMA,C3A,C2A	SC3_6	CMA,C3A,C2A	SC3_6
C3D,C2D,CMD	SC3_7	C3D,C2D,CMD	SC3_7
C2C,C3C	SC3_8	CMC,C2C,C3C	SC3_8
CAD,OBD	SC5_1	CAD,OBD	SC5_1
CMC,OMC	Na_1		
CBD,CGD,O1D	Na_2	CBD,CGD,O1D	Na_1
O2D,CED	Na_3	O2D,CED	Na_2
CGA,O1A,O2A	Na_4	CGA,O1A,O2A	Na_3
CBA,CAA	C2_2	CBA,CAA	C2_2
C1,C2,C3,C4,C5	C3_1	C1,C2,C3,C4,C5	C3_1
C6,C7,C8,C9,C10	C1_1	C6,C7,C8,C9,C10	C1_1
C11,C12,C13,C14,C15	C1_2	C11,C12,C13,C14,C15	C1_2
C16,C17,C18,C19,C20	C1_3	C16,C17,C18,C19,C20	C1_3

Table 3 AA to CG mapping for Chl *b* and Chl *a*.

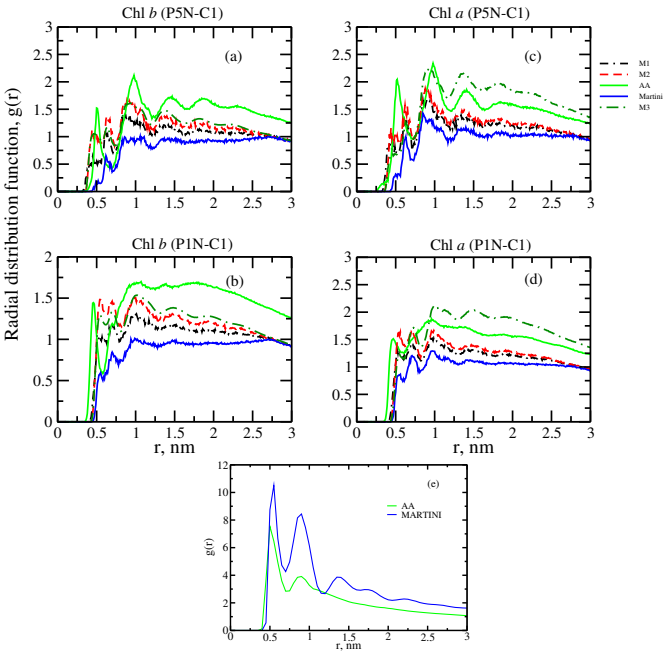

Figure S2 (a)-(d) Comparison of radial distribution functions (RDF) between central bead, Mg (bead type, P5N)/N (bead type P1N) and the atoms in the lipid tails (bead type C1). Plot shows clearly that the first peaks from models M1 and M2 are closer to the AA one than that of Martini. (e) RDF of lipid head groups from AA and MARTINI. The peaks of RDF are not reproduced well from MARTINI except the first peak.

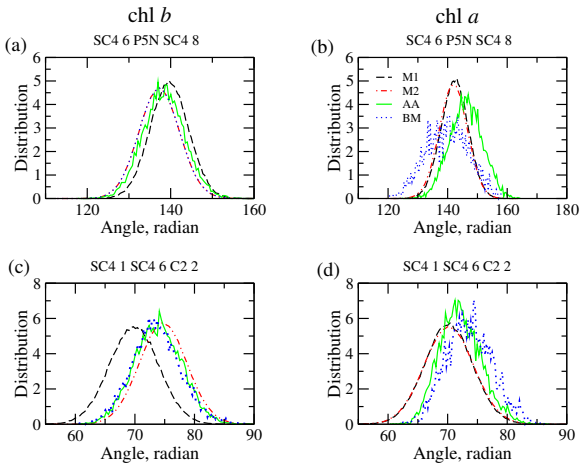

Figure S3 Conformational behavior of chl *b* and chl *a* obtained form the different CG models, as well as in the atomistic reference simulation. Panels (a) and (b) show the distribution of the angle between the CG beads SC4_1, SC4_6 and C2_2 of chl *b* and chl *a*, respectively. This angle characterizes the bending of the porphyrin ring system. Panels (c) and (d) show the distribution of the angle between the CG beads SC4_5, SC4_6 and SC4_1. This angles characterizes the orientation of the aliphatic tail with respect to the ring system. Color code: black dashed line – CG model M1, red dash-dotted line – CG model M2, green – atomistic reference, blue – atomistic ensemble after backmapping. It can be seen that both CG models reproduce the conformational behavior observed in the atomistic simulations well.

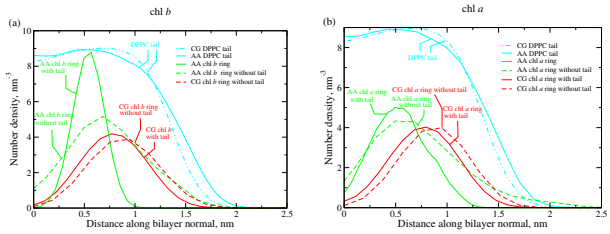

Figure S4 Number density distributions of the beads of the ring region of chl *b*/chl *a* in the DPPC bilayer are shown with respect to the absolute value of the distance normal to the bilayer. The maximum of the density distribution is shifted towards the polar head groups of the lipid bilayer in both the AA and CG levels of resolution for the porphyrin system without aliphatic tail. Thus, the tail of chl *b*/chl *a* helps the molecule to solvate better in the apolar hydrophobic region of the lipid bilayer.

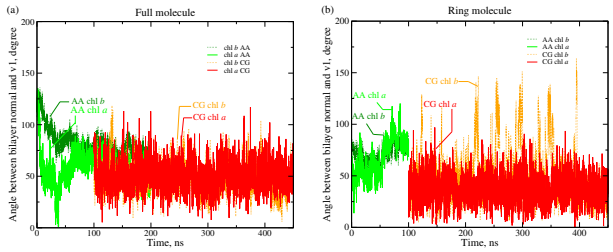

Figure S5 The time series of the angle between the vector **v1** and the bilayer normal (a) molecules with tail and (b) without tail. Solid line - chl *a*, dashed line - chl *b*. The angle for CG chl *a* ring without the tail fluctuates more than that of the ring with tail.

2 FRET experiments of chl in bilayers

2.1 Preparation of chl-containing liposomes

Chl *b* and *a*, isolated and separated as described previously[1] were dissolved in chloroform and added to the lipid 1,2-dipalmitoyl-sn-glycero-3-phospho-(1'-rac-glycerol (DPPG) (Avanti Polar Lipids, Alabaster, USA) at a lipid-to-chlorophyll-ratio (LCR) of 60. The solution was dried in a rotary evaporator (1 h, 30-70 mbar, RT) and the resulting lipid film hydrated in buffer (10 mM Tris/HCl (pH 7.5), 50 mM NaCl, 0.1 mM EDTA, lipid concentration 1.25 mg ml^{-1}) under vigorous vortexing. Unilamellar liposomes of about 100 nm in size were obtained by intense ultrasonication (Vibra Cell, Sonics & Materials, Newtown, USA) and two freeze-thaw-cycles followed by extrusion of the lipid suspension (LiposoFast, Avestin, Ottawa, Canada) through a polycarbonate membrane. Dilution with buffer and various amounts of liposomes without chlorophylls, followed by the described procedure for preparing unilamellar liposomes, yielded samples with LCR values between 150 and 25,000. About 60 % of the initially added Chls were lost during the procedure; this was taken into account when estimating the final LCR.

2.2 Aggregation-related fluorescence quenching

The fluorescence of Chl-containing liposomes at various LCRs was measured using a Fluoromax-2 spectrometer (Jobin Yvon, Bensheim, Germany) with the excitation wavelength set to 470 nm, 2 nm and 2 nm slit widths on the excitation and emission sides, respectively, and with signal corrections for fluctuations in the lamp intensity and for the wavelength dependence of the photon counter. The extinction of all samples was kept at less than 0.1. Quenching efficiencies (Q) in dependence on LCR were expressed as

$$Q = [F_b(LCR = 25,000) - F_b(LCR)]/F_b(LCR = 25,000),$$

where $F_b(LCR = 25,000)$ and $F_b(LCR)$ are the chl *b* fluorescence intensities at $LCR = 25,000$ and at the given LCR, respectively. The chl *b* and chl *a* fluorescence contributions were assessed by deconvoluting the measured fluorescence spectra into chl *b* and chl *a* spectra using reference spectra measured in DPPG and integrating the chl *b* and chl *a* spectra by using the rectangle rule.

The fluorescence quenching efficiency observed needed to be corrected for the contribution to chl *b* quenching by energy transfer from chl *b* to chl *a* in order to yield the fraction due to aggregation. Energy transfer was calculated by relating the sensitized acceptor emission with the correspondent fluorescence quantum yields (Φ_F) of the pigments (determined as described below):

$$Q_{ET}(LCR) = F_a(LCR) * \Phi_F^{chlb}/\Phi_F^{chla}$$

with $Q_{ET}(LCR)$ being the part of chl *b* fluorescence that is quenched due to energy transfer from chl *b* to chl *a*, and $F_a(LCR)$ being the chl *a* contribution to the fluorescence, both at the given LCR. $F_a(LCR)$ needed not to be corrected for

$F_a(LCR = 25,000)$ as direct excitation of chl *a* at the chosen excitation wavelength was negligible.

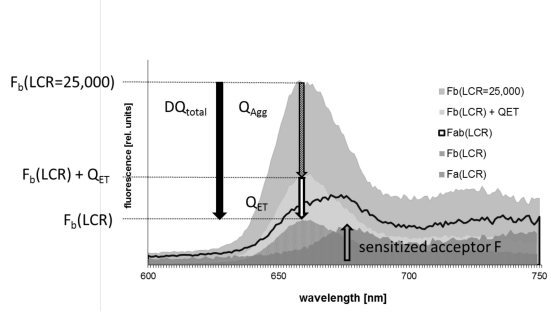

Figure S6 Schematic overview on quenching and energy transfer events. Quenching and energy transfer events in exemplary sample (LCR) compared to sample where neither aggregation nor energy transfer from chl *b* to chl *a* are thought to take place (LCR=25,000). Fb(LCR=25,000): chl *b* fluorescence intensities at LCR=25,000, Fab(LCR): fluorescence at given LCR, Fb(LCR): chl *b* fluorescence intensities at given LCR, Fa(LCR): chl *a* fluorescence intensities at given LCR, DQtotal: chl *b* quenching at given LCR compared to LCR=25,000, QAgg: chl *b* quenching by pigment aggregation, QET: chl *b* quenching by energy transfer from chl *b* to chl *a*.

In order to estimate the effect of aggregation of chl *a* on these calculations, assuming that fluorescence quenching due to aggregation affected chl *b* and chl *a* to the same extent, energy transfer efficiency was also estimated from comparing the chl *b* and chl *a* contributions. The relative contributions at LCR=25,000 were taken to reflect the situation at an energy transfer efficiency $ET = 0$. Then at a given $ET = x$, the initial chl *b* fluorescence F0 at LCR = 25,000 should be quenched to $F_x(chlb) = (1-x) * F_0(chlb)$. At the same time, the sensitized acceptor emission of chl *a* at an energy transfer efficiency of x is expected to be $x * F_0(chlb) * (qF(chla)/qF(chlb))$. Thus, for any observed ratio of chl b and chl a fluorescence intensity, the corresponding energy transfer efficiency ET = x could be calculated. Comparison of the values obtained by the different methods showed the effect of chl a aggregation on the calculated energy transfer efficiency to be insignificant.

2.3 Fluorescence quantum yields of chl b and a in liposomes

Fluorescence quantum yields (Φ_F) of chl *a* and chl *b* in a lipid environment were determined in references of LCR=1,875 in 1-palmitoyl-2-oleoyl-sn-glycero-3-phospho-1'-rac-glycerol (POPG) (Avanti Polar Lipids, Alabaster, USA) by the method described in Gundlach et al.[2] (excitation wavelength $\lambda_{ex} = 618$ nm, other settings and corrections as described) and using the published value for chl *a* in ethanol of 0.22 as reference[3]. They were 0.17 for chl *a* and 0.15 for chl *b*.

References

[1] P. Booth and H. Paulsen, *Biochem.*, 1996, **35**, 5103.

[2] K. Gundlach, M. Werwie, S. Wiegand and H. Paulsen, *Biochim. Biophys. Acta, Bioenerg.*, 2009, **1787**, 1499.

[3] G. Weber and F. W. J. Teale, *Trans. Faraday Soc.*, 1957, **53**, 646.